Int J Earth Sci (Geol Rundsch) (2017) 106:617–630
DOI 10.1007/s00531-016-1326-z

ORIGINAL PAPER

Elemental and Sr–Nd isotopic geochemistry of Permian Emeishan flood basalts in Zhaotong, Yunnan Province, SW China

Juan Li[1,2] · Hong Zhong[1] · Wei-Guang Zhu[1] · Zhong-Jie Bai[1] · Wen-Jun Hu[1]

Received: 19 November 2015 / Accepted: 3 April 2016 / Published online: 4 May 2016

Abstract This study presents new whole-rock elemental and isotopic data for the basalts from the Zhaotong area, located in the intermediate zone of the ~260 Ma Emeishan large igneous province (ELIP). The Zhaotong basalts belong to high-Ti series with TiO_2 from 2.93 to 5.26 % and Ti/Y from 519 to 974. The parental magma was subjected to minor crustal contamination as indicated by slight Nb–Ta depletion (Nb/La: 0.72–1.10). Meanwhile, the relatively invariable Sr–Nd isotopes ($\varepsilon_{Nd}(t)$: −0.74 to +2.86, mostly +1.10 to +2.86; $(^{87}Sr/^{86}Sr)_i$: 0.7050–0.7072) and the light rare earth elements (LREE) enrichment (La/Yb: 10.3–19.1) of the basalts prefer a mantle plume origin. A garnet-dominated peridotite mantle source was further suggested on the basis of the REE distribution patterns and high Sm/Yb and high La/Yb ratios. This study further confirms the geochemical zoning of the high-Ti basalts in the ELIP, which is in accordance with both the spatial distribution and the thickness of the basalts. The high-Ti basalts in the intermediate and outer zones of ELIP (e.g., Zhaotong and Guizhou) share similar Sr–Nd isotopic and elemental compositions, suggesting that they originated directly from the Emeishan mantle plume. By contrast, the high-Ti basalts in the inner zone (e.g., Longzhoushan and Binchuan) have variable compositions, indicating a rather heterogeneous mantle source possibly involved with subcontinental lithospheric mantle (SCLM) components.

Keywords High-Ti basalts · Sr–Nd isotopes · Emeishan large igneous province · SW China

Introduction

The Emeishan flood basalts and associated mafic–ultramafic and felsic intrusions, recognized as an important large igneous province (LIP) in China, have long been the focus of stratigraphic, geochronological, geochemical and geophysical studies. Evidence from sedimentary sequences below the Emeishan basalts, geophysical investigation, radiometric datings, petrology of the basalts and their related rocks in the Emeishan LIP (ELIP) strongly supports a mantle plume origin (Chung and Jahn 1995; Xu et al. 2001, 2004; Xu and He 2007; Song et al. 2001, 2004, 2006, 2008, 2009; Hao et al. 2004; Zhong et al. 2002, 2006, 2011; Zhou et al. 2002; Xiao et al. 2003, 2004; He et al. 2003; Ali et al. 2005; Zhang et al. 2006, Zhang 2009; Wang et al. 2007; Fan et al. 2008; Qi et al. 2008; Qi and Zhou 2008; Lai et al. 2012; Zhong et al. 2014; Chen et al. 2015; Xu et al. 2015). The basalts in the ELIP have been generally divided into two major magma series: high-Ti series (TiO_2 > 2.5 %, Ti/Y > 500) and low-Ti series (TiO_2 < 2.5 %, Ti/Y < 500) (Xu et al. 2001). Moreover, based on biostratigraphy, sedimentology and geochemistry, the ELIP has been subdivided into the inner, intermediate and outer zones (Fig. 1), which also corresponds to crustal thickness (He et al. 2003; Xu et al. 2004; Shellnutt and Jahn 2011; Xu et al. 2015). The inner zone with thickest crust (55–64 km) comprises both high-Ti series and low-Ti

Electronic supplementary material The online version of this article (doi:10.1007/s00531-016-1326-z) contains supplementary material, which is available to authorized users.

✉ Hong Zhong
zhonghong@vip.gyig.ac.cn

[1] State Key Laboratory of Ore Deposit Geochemistry, Institute of Geochemistry, Chinese Academy of Sciences, 99 West Lincheng Road, Guiyang 550081, China

[2] University of Chinese Academy of Sciences, Beijing 100049, China

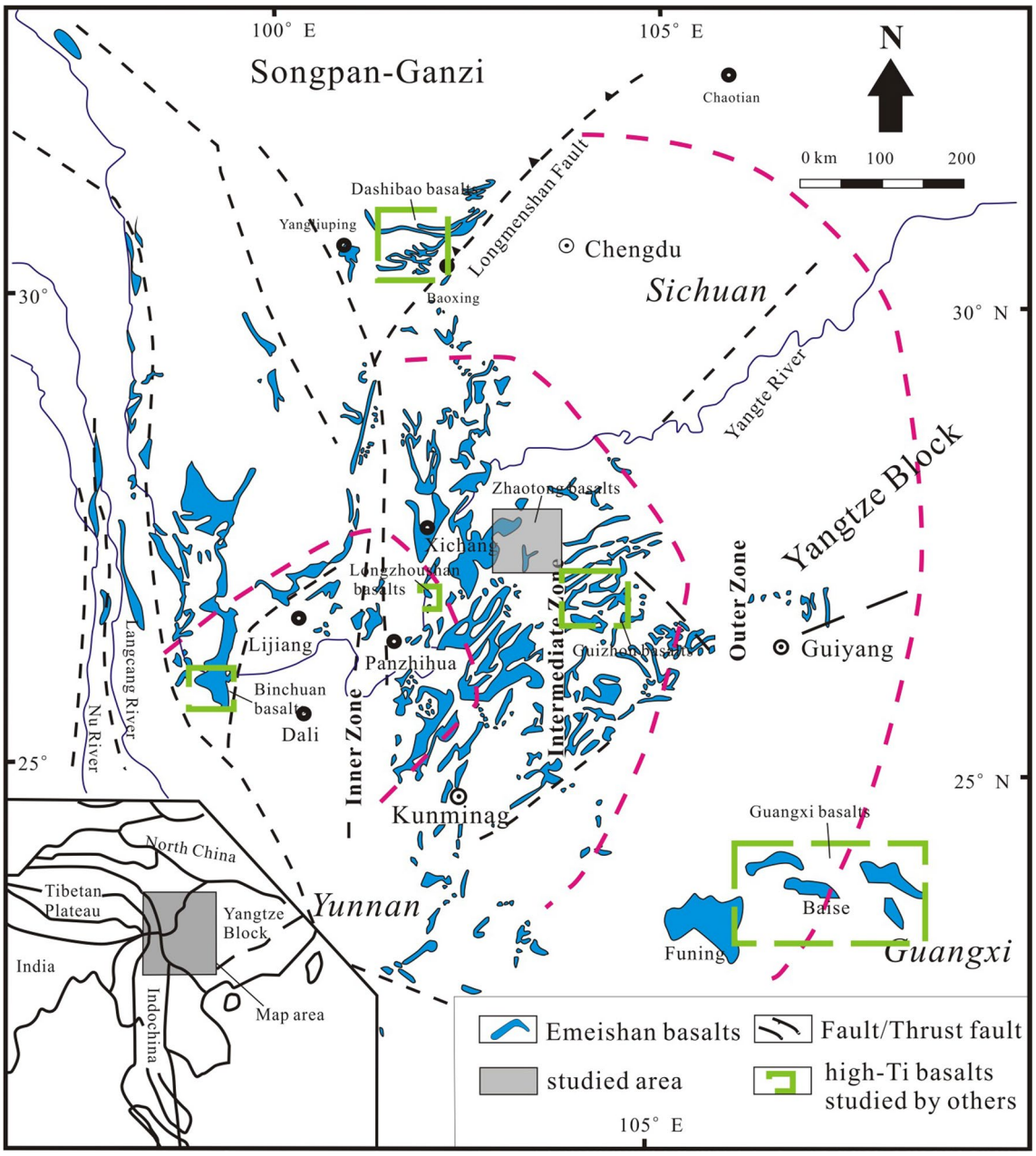

Fig. 1 Simplified geological map showing the distribution of the Emeishan basalts (modified after He et al. 2003; Zi et al. 2010). Samples were collected from the Zhaotong area, northeastern Yunnan Province

series with a diversity of rock types (e.g., picrites, basalts, basaltic pyroclastic rocks, and basaltic andesites) (Xu et al. 2001, 2004; Xiao et al. 2004), while the intermediate zone (38–54 km) and outer zone (35–43 km) with thinner crust mainly consist of high-Ti basalts (Xu et al. 2004).

Numerous geochemical studies have demonstrated that the high-Ti rocks and low-Ti rocks of the ELIP might originate from different mantle sources under variable melting conditions (Chung and Jahn 1995; Xu et al. 2001, 2004; Xiao et al. 2004). In general, the low-Ti basalts are considered to originate from larger degrees of partial melting at a lower depth and involve more crustal materials than the high-Ti basalts (Xu et al. 2001; Xiao et al. 2004). However, the genesis of high-Ti basalts is still debatable (Xu et al. 2001; Song et al. 2001, 2008; He et al. 2003; Xiao et al. 2004; Ali et al. 2005). For instance, some authors argued that the high-Ti magma was directly generated from the head of the Emeishan mantle plume by large scale and low degrees of partial melting (Xiao et al. 2004), whereas others suggested that the high-Ti basaltic magma most likely originated from

a SCLM reservoir or was mixed with a significant amount of lithospheric mantle material during the ascent of plume-related magma through the SCLM (Xu et al. 2007).

In comparison with numerous studies in the inner ELIP (Xu et al. 2001, 2004; Xiao et al. 2004), relatively limited researches were conducted on the intermediate and outer zones of the ELIP, especially in the northeast of Yunnan Province. To further understand the genesis of the high-Ti basalts, we have conducted a systematic study on the Zhaotong basalts located in the intermediate zone of the ELIP in this paper. The results suggest that the parental magmas of the Zhaotong basalts originated from a garnet peridotite mantle source by low degrees of partial melting. Meanwhile, a comparison of our samples with the high-Ti basalts from other areas of the ELIP provides new insights into the high-Ti basalts from different zones of the ELIP. The high-Ti basalts in the intermediate and outer zones of ELIP are suggested to originate from a homogenous mantle plume, while the high-Ti basalts in the inner zone indicate a rather heterogeneous mantle source possibly involved with SCLM components.

Geological background and petrography

The ELIP crops out in the western Yangtze Block, exposed in a rhombic province of over 500,000 km^2 in Yunnan, Sichuan and Guizhou provinces (Xu et al. 2001, 2004; Ali et al. 2005) (Fig. 1). Some basalts and mafic complexes exposed in the Simao basin, northern Vietnam and Qiangtang terrain are possibly an extension of the ELIP (Chung et al. 1998; Xiao et al. 2004). The Yangtze Block consists of Precambrian basement and a thick sedimentary sequence of Sinian and Paleozoic clastic rocks and limestone, which are overlain by Triassic to Cretaceous continental and marine sedimentary rocks (Yan et al. 2003). The northwestern boundary of the ELIP is the Longmenshan thrust fault, and the southwestern is the Ailaoshan-Red River slip fault. The thickness of the entire volcanic sequence varies from 5 km in the west to a few hundred meters in the east. Recently, CA-TIMS zircon U–Pb dating of felsic ignimbrite from the Binchuan section indicates the termination age of ELIP is 259.1 ± 0.5 Ma, which is very close to the Guadalupian–Lopingian boundary (Zhong et al. 2014).

In addition to main picrites, tholeiites and basaltic andesites, the ELIP also contains numerous mafic–ultramafic and syenitic–granitic intrusions, some of which host giant Fe–Ti–V oxide deposits (Zhou et al. 2005). The basalts in Zhaotong are located in the northeast of Yunnan Province and belong to the intermediate zone of the ELIP (He et al. 2003; Xu et al. 2004). Besides, the Zhaotong basalts are unconformably underlain by limestones of the Lower Maokou Formation, and in turn conformably covered by the Upper Permain Xuanwei Formation composed of mudstone, sandstone and conglomerate with interbedded coal seams.

We systematically collected 89 basalts samples from the Zhaotong area. Some sampled basalts exhibit typical porphyritic and vesicular textures with groundmass of intergranular or intersertal texture and phenocryst of plagioclase or clinopyroxene. The most common phenocrysts are tabular plagioclases of variable percentages (5–25 %), locally accompanied with sparse clinopyroxene (<5 %) and olivine (<5 %). The groundmass is fine grained and composed of plagioclase (20–50 %), clinopyroxene (10–20 %), basaltic glass (30–50 %) and minor Fe–Ti oxides (<5 %). Some samples have amygdaloidal texture that variable vesicles are filled with chlorite. Moreover, some samples are aphyric and the whole rocks are mainly composed of plagioclase (50–60 %), clinopyroxene (25–30 %), Fe–Ti oxides (magnetite and ilmenite) (5–10 %) and olivine (<5 %). In general, our samples are fresh with only minor chlorite along the fractures.

Analytical methods

Fresh rock chips were powdered to 200-mesh size using a tungsten carbide ball mill. Whole-rock major oxides were determined by ME-XRF 06d method in the ALS (Guangzhou) laboratory. The analytical accuracy for major oxides present in concentrations is better than 5 %. Trace elements were determined using inductively coupled plasma mass spectrometer (ICP–MS) at the Institute of Geochemistry, Chinese Academy of Sciences. The powdered samples (50 mg) were dissolved in high-pressure Teflon bombs using HF + HNO_3 mixture for 48 h at ~190 °C (Qi et al. 2000). Rh was used as an internal standard to monitor signal drift during counting. The analytical precision is generally better than 5 %.

The whole-rock Sr–Nd isotopes were determined on a MC-ICP-MS at the Institute of Geochemistry, Chinese Academy of Sciences. The analytical procedures are as follows: Approximately 120 mg of sample powders were weighed into Teflon bombs and dissolved on a hotplate using HF, HNO_3 and $HClO_4$ at 20 °C for a week. After dissolution of the sample, the solution was totally dried. 6 mol/L HCl was then added and evaporated to dryness (twice). The residue was dissolved with 1.5 mL HCl of 2.5 mol/L. After centrifugal separation, 1 mL supernatant was passed through a cation-exchange resin (AG50 W × 12), and 5 mol/L HCl to elute Sr. 6 mol/L HCl was then used to elute rare earth elements

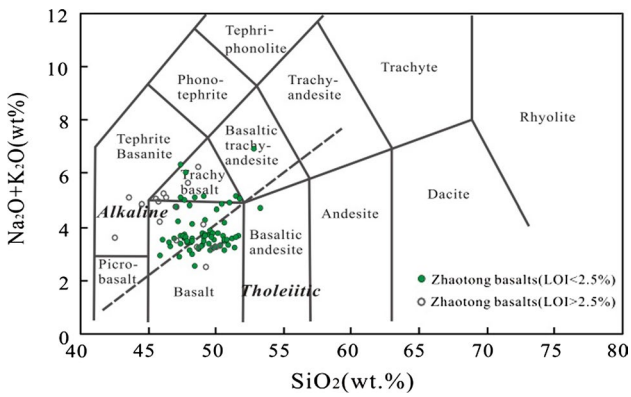

Fig. 2 Total alkalis–silica (TAS) diagram of the Emeishan high-Ti basalts in Zhaotong. The *bold dashed line* distinguishes tholeiitic from alkaline basalts (from MacDonald and Katsura 1964)

(REEs), and the solution was dried. 0.1 mol/L HCl was passed through up REE on an anion-exchange resin (P507), and then, 0.2 mol/L HCl was added to elute Nd. Mass fractionation corrections for Sr and Nd isotopic ratios were based on values of $^{86}Sr/^{88}Sr = 0.1194$ and $^{146}Nd/^{144}Nd = 0.7219$. The Sr standard solutions (NBS 987) were analyzed eight times and yield $^{87}Sr/^{86}Sr$ ratio of 0.710261 ± 18 (2σ). The Nd standard solution (JnDi) was also analyzed eight times and has an $^{143}Nd/^{144}Nd$ ratio of 0.512116 ± 12 (2σ). The measured results for the USGS standard BCR-2 were $^{87}Sr/^{86}Sr = 0.705299 \pm 20$ (2σ) and $^{143}Nd/^{144}Nd = 0.512658 \pm 7$ (2σ).

Analytical results

Major elements

Elemental data for the Zhaotong samples are listed in Appendix A for ESM. Consistent with petrographic observation, the samples display some alteration features, as reflected by loss on ignition (LOI) ranging from 0.24 to 5.97 %. Thus, the samples with LOI less than 2.5 % were chosen for major and trace element study. The samples from Zhaotong are mainly plotted in the basalt field on the total alkalis–silica (TAS) diagram (Fig. 2), with SiO_2 ranging from 45.9 to 53.3 % and MgO from 2.85 to 5.62 % with an average value of 4.29 %. All the analyzed samples have TiO_2 contents of 2.93–5.26 % and Ti/Y ratios of 519–974, therefore, belonging to the high-Ti basalt group (Xu et al. 2001). The contents of the Al_2O_3 and Fe_2O_3 correlate positively with MgO contents, while SiO_2 and TiO_2 correlate negatively with MgO (Fig. 4). These geochemical characteristics suggest that these basalts were not derived from primary magma and must have undergone fractional crystallization processes.

Trace elements

The collected basalts in Zhaotong have high large ion lithosphere elements (LILE) and high field strength element (HFSE) contents (Appendix A for ESM). The samples have La of 27–54.3 ppm, Sm of 6.66–13.5 ppm and Yb of 2.18–3.18 ppm. The La/Yb ratios of the basalts range from 10.3 to 19.1 and Sm/Yb from 2.5 to 4.5. Thus, they are strongly enriched in light REE (LREE) relative to heavy REE (HREE) and display moderately sloping HREE on chondrite-normalized patterns (Fig. 3a). Besides, all samples have similar primitive mantle-normalized trace element patterns showing enrichment in LILE (Fig. 3b), such as Ba, Th and U. Most samples show features similar to enriched ocean island basalts (OIB) except Sr depletion and slight depletion in Nb and Ta (Nb/La: 0.72–1.1). In addition, only several samples show negative Eu anomalies, and most samples show positive Eu anomalies (Eu/Eu*:0.88–1.33, mostly >1.0). The Sr/Sr* ratios show positive correlations with MgO (Fig. 5), which might be caused by fractionation of plagioclase. The contents of Ni and Cr are low (Ni: 1.80–131 ppm, Cr: 20.5–103 ppm). Meanwhile, both Ni and Cr values correlate positively with MgO contents (Fig. 4).

Rb–Sr and Sm–Nd isotopic compositions

Sr and Nd isotopic ratios and abundances are given in Table 1. The initial isotopic compositions have been calculated to 260 Ma. The Nd isotopic compositions of the Zhaotong basalts are relatively invariable with initial $^{143}Nd/^{144}Nd$ ratios ranging from 0.5123 to 0.5125 (mostly 0.5124) and ε_{Nd} (t) values ranging from -0.74 to $+2.86$. The ε_{Nd} (t) values and initial $^{87}Sr/^{86}Sr$ ratios of most samples are within the range of the ELIP from previous studies distinct from depleted mantle (DM) and the Emeishan low-Ti picrites (Xiao et al. 2004; Qi et al. 2008; Qi and Zhou 2008; Wang et al. 2007; Song et al. 2008; Lai et al. 2012) (Fig. 6).

Discussion

Crustal contamination and fractional crystallization

The Nb–Ta depletion in the Zhaotong basalts suggests contributions of continental crust, which can be explained by either assimilation during fractional crystallization or incorporation of crustal materials into the source. Distinguishing these two processes is essential for our knowledge of the mantle–crust interaction and the genesis of the basalts in the ELIP. One commonly used method is the relations between indexes of magma fractionation and

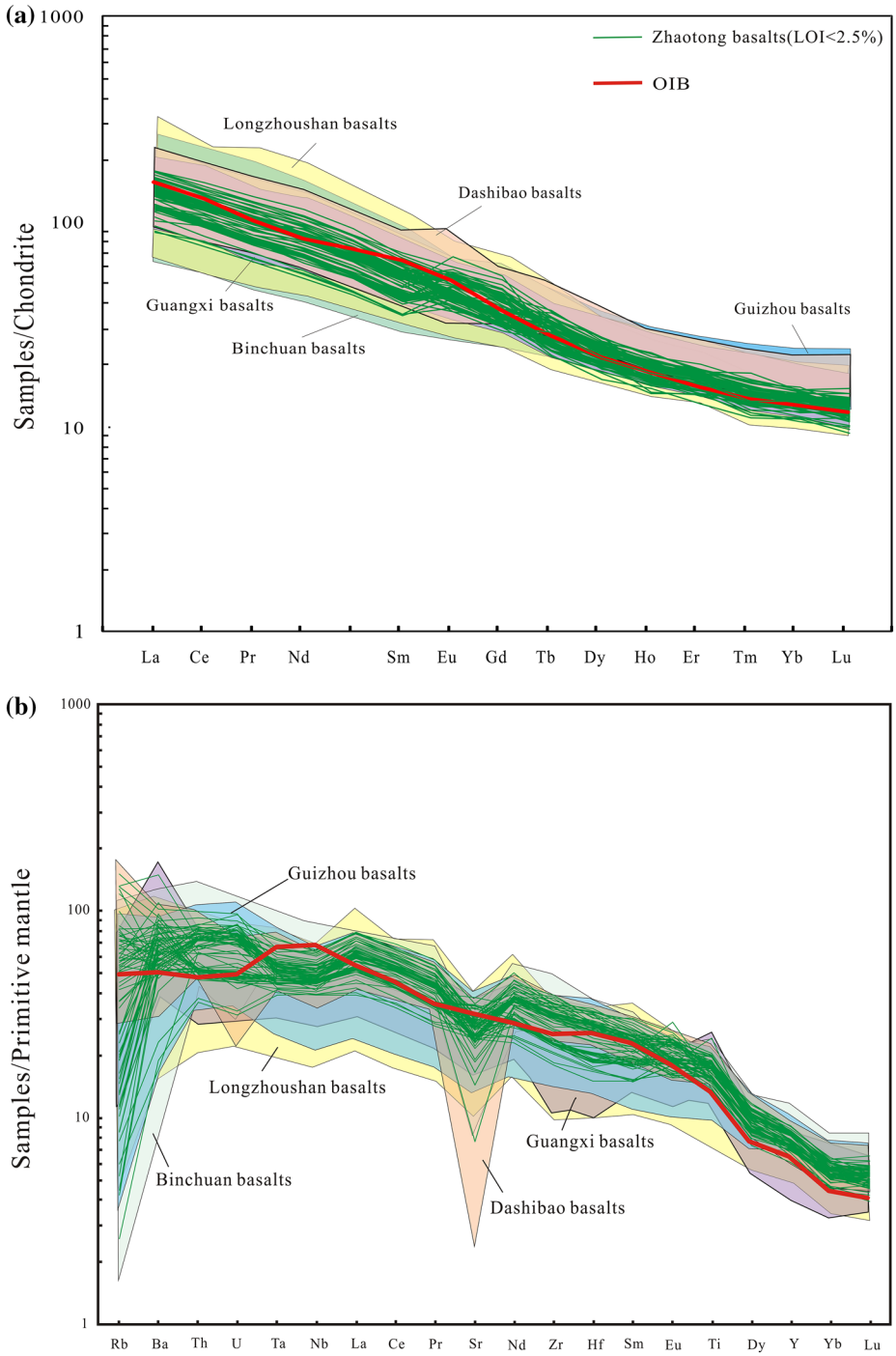

Fig. 3 **a** Chondrite-normalized REE patterns for the Zhaotong basalts. **b** Primitive mantle-normalized, incompatible trace element patterns for the flood basalts in Zhaotong. The chondrite values are from Sun and McDonough (1989). Data of the Binchuan samples are from Xiao et al. (2004). The Guangxi samples are from Lai et al. (2012) and Fan et al. (2008). The Guizhou samples are from Qi and Zhou (2008). The Longzhoushan samples are from Qi et al. (2008). The Dashibao samples are from Zi et al. (2010)

whole-rock isotopes or trace elements ratios (Bezard et al. 2014; Jahn et al. 1999). As shown in Fig. 7, the ratios of Nb/La decrease with the decreasing MgO and show slightly positive correlation with $\varepsilon_{Nd}(t)$. In other words, the Nb–Ta depletion developed with the isotopic variations during the magma fractionation. These features indicate some crustal contamination in the Zhaotong basalts. On the other hand, the available isotopic data could help us to constrain the degree of crustal contamination (Fig. 6). The Nd isotopic compositions of these basalts show limited variations with the initial $^{143}Nd/^{144}Nd$ ratios ranging from 0.5123 to 0.5125 and $\varepsilon_{Nd}(t)$ values ranging from −0.74 to +2.86 (mostly +1.10 to +2.86), indicating that the Zhaotong basalts underwent minor contamination (<10 %) by the Yangtze upper/middle crust (Wang et al. 2007).

Moreover, the Zhaotong basalts have low MgO (mostly < 7 %), $Mg^{\#}$ (28–48), Cr (<131 ppm) and Ni (<103 ppm) contents, suggesting that they represent

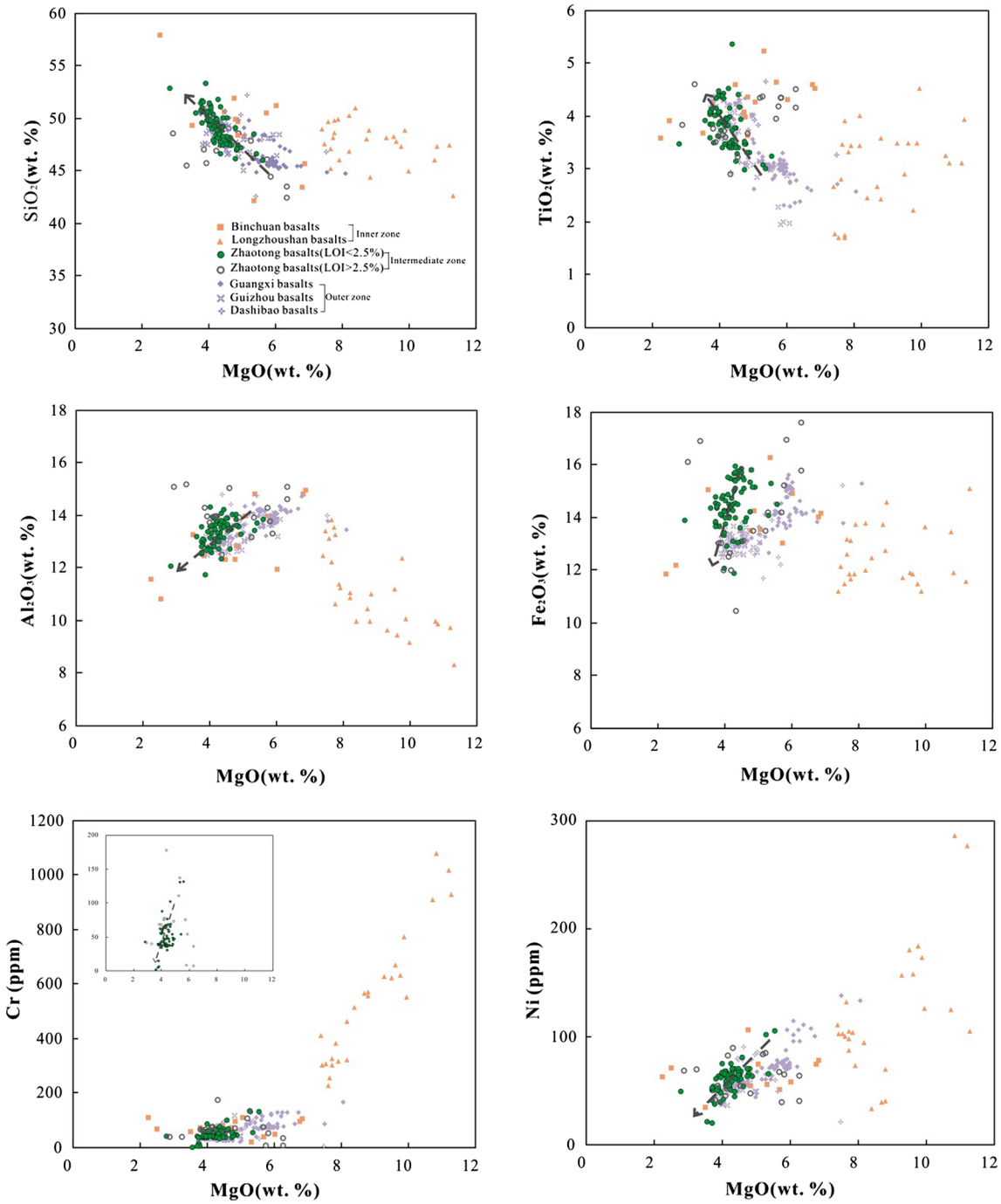

Fig. 4 Plots of MgO versus major oxides and selected trace elements for the Zhaotong basalts

relatively evolved magmas and in turn a significant mass fraction of more primitive rocks is yet to be sampled. As shown in Fig. 4, positive correlations between Ni and Cr with MgO indicate fractionation of olivine and clinopyroxene, which is corresponding to minor olivine and clinopyroxene phenocrysts in the basalts. The negative correlation between MgO and TiO_2 argues against fractionation of Ti–Fe oxides. However, considering the existence of minor Ti–Fe oxides in our collected samples, fractionation of Ti–Fe oxides might be insignificant in the evolution of the Zhaotong high-Ti magma. Al_2O_3 decreasing with decreasing of MgO and the presence of lots of plagioclase phenocrysts suggest extensive fractionation of plagioclase. Compared with other REEs that are highly incompatible for the plagioclase in basic magma with the partition coefficients are mostly <0.1, Eu is moderately

Table 1 Whole-rock Sr and Nd isotopic data for the Zhaotong basalts, Yunnan Province, SW China

Sample	Rb (ppm)	Sr (ppm)	$^{87}Rb/^{86}Sr$	$^{87}Sr/^{86}Sr \pm 2\sigma$	$(^{87}Sr/^{86}Sr)_i$	Sm (ppm)	Nd (ppm)	$^{147}Sm/^{144}Nd$	$^{143}Nd/^{144}Nd \pm 2\sigma$	$(^{143}Nd/^{144}Nd)_i$	$\varepsilon_{Nd}(t)$
ZT1501	48.8	491	0.2876	0.706790 ± 28	0.7057	11.2	30.0	0.2240	0.512645 ± 7	0.5123	−0.74
ZT1503	16.3	603	0.0782	0.705508 ± 15	0.7052	8.30	37.1	0.1346	0.512644 ± 6	0.5124	2.18
ZT1505	10.5	197	0.1542	0.706947 ± 17	0.7064	13.5	61.7	0.1313	0.512622 ± 5	0.5124	1.86
ZT1507	36.5	506	0.2087	0.706499 ± 16	0.7057	11.2	50.5	0.1329	0.512631 ± 7	0.5124	1.98
ZT1510	33.3	529	0.1821	0.706231 ± 14	0.7056	11.0	50.5	0.1308	0.512597 ± 7	0.5124	1.38
ZT1512	42.1	584	0.2086	0.706338 ± 17	0.7056	11.2	51.8	0.1295	0.512580 ± 6	0.5124	1.10
ZT1514	40.1	686	0.1691	0.706976 ± 24	0.7064	10.5	48.4	0.1308	0.512598 ± 6	0.5124	1.41
ZT1518	34.0	658	0.1495	0.706510 ± 15	0.7060	12.4	62.2	0.1200	0.512621 ± 7	0.5124	2.22
ZT1520	81.3	810	0.2904	0.707443 ± 22	0.7064	9.17	47.3	0.1167	0.512581 ± 5	0.5124	1.54
ZT1523	34.8	658	0.1530	0.706190 ± 13	0.7056	11.8	60.3	0.1178	0.512579 ± 5	0.5124	1.47
ZT1525	48.2	660	0.2113	0.706679 ± 25	0.7059	10.9	52.2	0.1257	0.512622 ± 6	0.5124	2.06
ZT1527	26.6	576	0.1336	0.706182 ± 34	0.7057	10.9	51.4	0.1276	0.512667 ± 9	0.5125	2.86
ZT1530	5.43	525	0.0299	0.707345 ± 42	0.7072	7.98	40.7	0.1180	0.512617 ± 9	0.5124	2.20
ZT1532	9.30	682	0.0395	0.705964 ± 25	0.7058	7.98	40.0	0.1200	0.512648 ± 6	0.5124	2.75
ZT1535	2.85	631	0.0131	0.705129 ± 13	0.7050	7.64	39.2	0.1173	0.512629 ± 8	0.5124	2.46
ZT1542	12.1	741	0.0473	0.705517 ± 19	0.7053	8.32	40.3	0.1242	0.512637 ± 7	0.5124	2.38
ZT1544	12.5	730	0.0495	0.705190 ± 14	0.7050	8.51	40.4	0.1268	0.512640 ± 7	0.5124	2.37
ZT1554	16.1	718	0.0649	0.705398 ± 26	0.7051	8.08	38.0	0.1279	0.512656 ± 6	0.5124	2.64
ZT1560	0.69	109	0.0183	0.705789 ± 15	0.7057	8.48	44.2	0.1154	0.512609 ± 6	0.5124	2.14
ZT1569	23.5	509	0.1336	0.706290 ± 15	0.7058	11.0	52.8	0.1254	0.512640 ± 6	0.5124	2.41
ZT1583	41.8	560	0.2160	0.705839 ± 22	0.7050	10.5	49.8	0.1269	0.512564 ± 7	0.5123	0.88
ZT1593	28.7	579	0.1434	0.706716 ± 13	0.7062	10.6	51.7	0.1234	0.512538 ± 4	0.5123	0.49
ZT1597	23.2	570	0.1178	0.706372 ± 11	0.7059	9.72	47.2	0.1239	0.512542 ± 4	0.5123	0.54
JnDi ($n = 8$)									0.512116 ± 12		
NBS987 ($n = 8$)				0.710261 ± 18							
BCR-2	48.9	377		0.705299 ± 20		6.02	28.80		0.512658 ± 7		

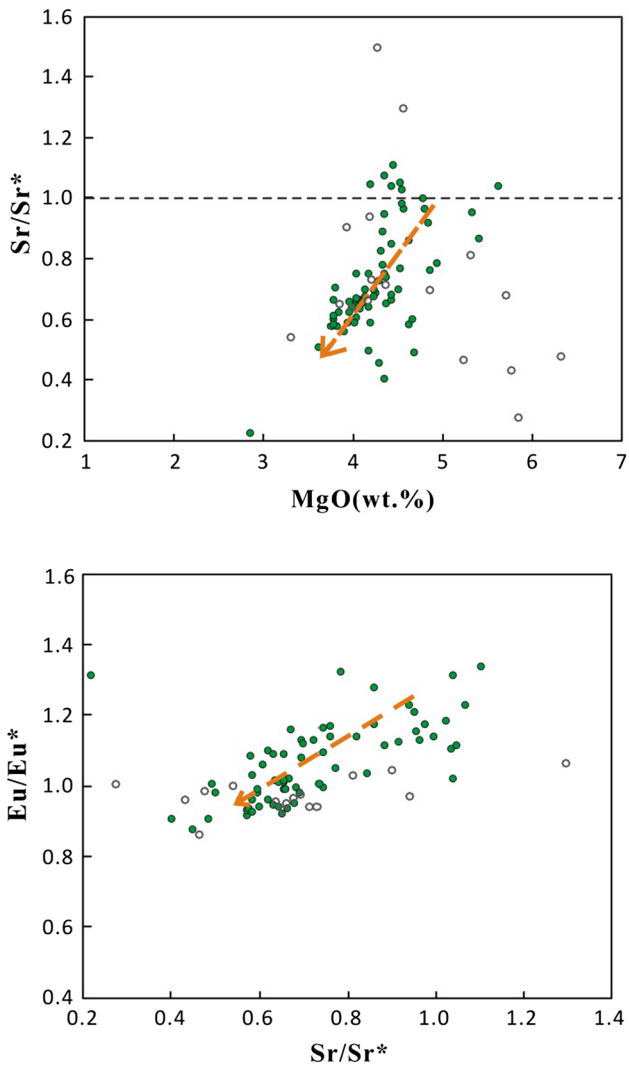

Fig. 5 Plots of MgO versus Sr/Sr* and Eu/Eu* versus Sr/Sr*

incompatible ($D_{plagioclase/melts}$ = 0.55) and Sr is compatible ($D_{plagioclase/melts}$ = 2.0) (McKenzie and O'Nions 1991). Therefore, the positive correlations between Eu/Eu* versus Sr/Sr* and Sr/Sr* versus MgO (Fig. 5) also suggest the extensive fractionation of plagioclase. The slightly positive Eu anomalies in these evolved lavas might reflect a high Eu^{3+}/Eu^{2+} ratio in the magma (Frey et al. 1993; Xu et al. 2001; Xiao et al. 2004). The negative Sr anomalies might be mainly caused by fractional crystallization of plagioclase in the magma chamber or during magma ascent and thus may not give information about source components.

Mantle source and partial melting

Understanding the petrogenesis of basaltic magmas involves estimating their source compositions, degrees of partial melting and the processes that took place during their ascent and eruption (Qi and Zhou 2008). The Zhaotong high-Ti basalts have elemental patterns (Fig. 3a, b) and $\varepsilon_{Nd}(t)$ values (−0.74 to +2.86, Fig. 6) typical of an OIB mantle source. Besides, the Zhaotong basalts have higher Nb (26.6–51.2 ppm) and Zr (201–491 ppm) contents, which are comparable with those of OIB (Nb = 48, Zr = 280 ppm), but much higher than those of the N-MORB (Nb = 2.33, Zr = 74 ppm), suggesting that these basalts were derived from an OIB-like mantle source.

The degree of partial melting is difficult to estimate because the source composition is unknown. However, REE abundances and ratios of the basalts are still helpful to estimate the composition of the mantle source and degree of partial melting. The partition coefficients between garnet and melt increase steadily from highly incompatible for the LREE to moderately compatible for the HREE (Hellebrand et al. 2002), so that Sm versus Sm/Yb and La/Sm versus Sm/Yb diagrams can be used to distinguish between melting of spinel and garnet peridotite. When a spinel peridotite undergoes partial melting, the ratios of La/Sm and Sm/Yb are only slightly fractionated. In contrast, small degrees of partial melting of a garnet peridotite source will produce melts with significantly high La/Sm and Sm/Yb ratios (Aldanmaz et al. 2000). The La/Sm and Sm/Yb values for the Zhaotong basalts are extremely high (La/Sm: 3.5–4.8; Sm/Yb: 2.5–4.5). In the diagram of Sm versus Sm/Yb, the rocks of the high-Ti series are displaced from the spinel-lherzolite melting trend to higher Sm/Yb ratios and plot between the melting trajectories for garnet-lherzolite and garnet + spinel-lherzolite, indicating that the high-Ti series was derived from a garnet-dominated bearing mantle source (Fig. 8a). The trend shown by the La/Sm versus Sm/Yb plot (Fig. 8b) also agrees with a garnet-lherzolite mantle source.

Low degree of partial melting to form the basalts could be constrained by the high concentrations of incompatible elements in the Zhaotong high-Ti basalts. Meanwhile, the basalts have low Al_2O_3/TiO_2 ratios (2.5–4.7 compared with ~20 in primitive mantle) and high $(Sm/Yb)_N$ ratios (2.7–5.0), indicating small degrees of partial melting of relatively deep mantle source. Xu et al. (2001) proposed that the parental magmas of the HT lavas were produced by a small degree (1.5 %) of partial melting. Further, Zhang et al. (2006) studied Lijiang high-Ti picritic lavas that are commonly considered to be directly extracted from the mantle reservoir without significant subsequent differentiation and suggested they melted in the presence of garnet and with rather small amounts of partial melting of ~2–7 %. As shown in Fig. 8a, our samples suggest the degree of partial melting is <8 %.

Geochemical features of the high-Ti basalts in the ELIP

In the ELIP, the geochemical features of the high-Ti basalts are complex. For instance, Xu et al. (2001) suggested that

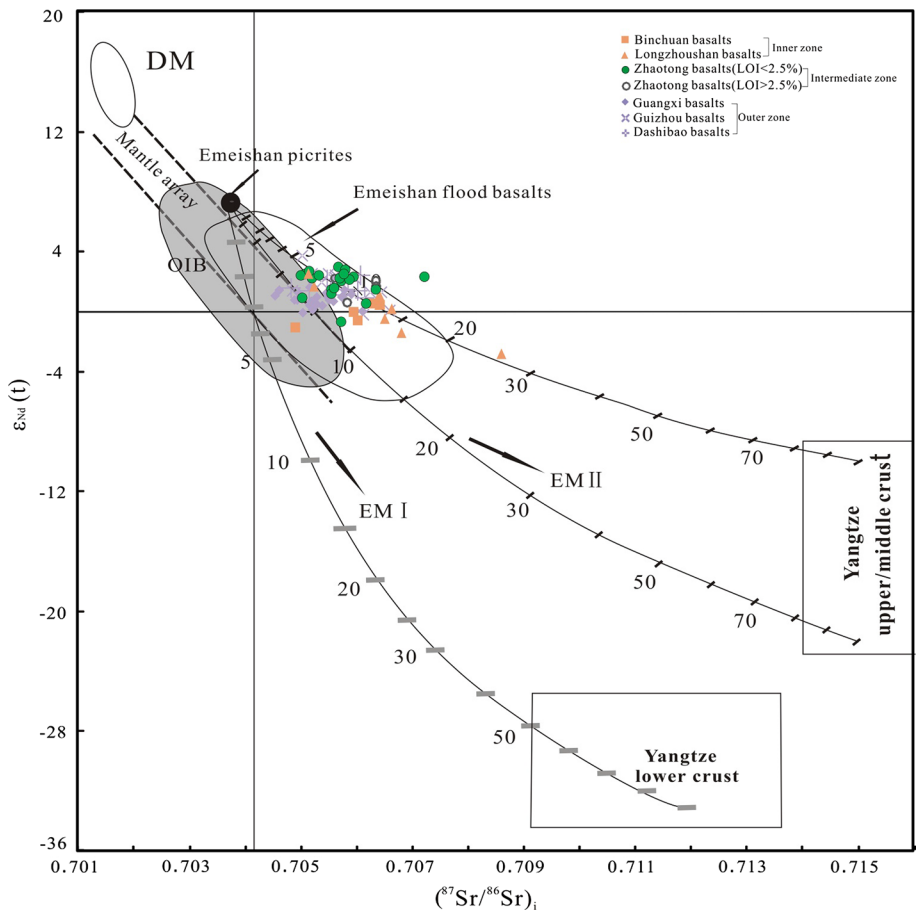

Fig. 6 $\varepsilon_{Nd}(t)$ ($t = 260$ Ma) values versus $(^{87}Sr/^{86}Sr)_i$ diagram for the Emeishan high-Ti basalts from Zhaotong. DM (depleted mantle), mantle array and EMI and EMII trends are after Zindler and Hart (1986). OIB data are from Wilson (1989). The Yangtze upper/middle crust and lower crust data are from Gao et al. (1999), Ma et al. (2000) and Chen and Jahn (1998). The numbers indicate the percentages of participation of the crustal materials. The data of the Emeishan basalts are from Xu et al. (2001) and Xiao et al. (2004)

the high-Ti basalts can be further divided into three subtypes: HT1 ($TiO_2 > 3.6$ %, $Mg^{\#} < 45$), HT2 ($TiO_2 < 2.5$–3.5 %, $Mg^{\#} < 45$–52) and HT3 ($Mg^{\#} = 51$–61, differ from low-Ti with higher TiO_2 at comparable $Mg^{\#}$) and show distinct geochemical features in different zones. Meanwhile, He et al. (2010) suggested that the high-Ti basalts in peripheral zone have slightly narrower ranges of $\varepsilon_{Nd}(t)$ values than the high-Ti basalts in the central and western zones. Hence, we attempt to integrate these previous studies (Qi and Zhou 2008; Qi et al. 2008; Lai et al. 2012; Fan et al. 2008; Xiao et al. 2004; Zi et al. 2010) along with our new data to provide more insights into the genesis of the Emeishan high-Ti basalts. We illustrate that a certain difference exists between the high-Ti basalts in the intermediate/outer zones of the ELIP (e.g., Zhaotong, Guizhou, Guangxi and Dashibao) and those in the inner zone (e.g., Binchuan and Longzhoushan). The results are as follows:

1. The high-Ti basalts in the intermediate and outer zones mainly belong to HTI type (Xu et al. 2001) and share similar geochemical features characterized by considerable enrichment in LREE and LILEs, which are clearly different from typical N-MORB, but similar to OIB. Most of basalts show weak Nb–Ta depletion and obviously negative Sr anomalies. In addition, these high-Ti basalts have narrow Sr–Nd isotope ranges ($\varepsilon_{Nd}(t)$ from −0.74 to +3.68), indicating that they might originate from a homogeneous mantle source and experience limited crustal contamination. In plots of MgO versus major oxides and trace elements (Fig. 4), all the basalts have low MgO, Cr, Ni values and relatively high TiO_2 values. The values of Al_2O_3, Fe_2O_3, Cr and Ni show positive relationships with MgO values (except some samples in Dashibao) while SiO_2 and TiO_2 values correlate negatively with MgO values, indicating that the high-Ti basalts in the intermediate and outer zones of the ELIP are controlled by fractional crystallization of olivine + clinopyroxene + plagioclase.
2. In the inner part of the ELIP where the high-Ti basalts account for smaller portions than low-Ti basalts (Xu et al. 2001), the high-Ti basalts show several geochemical features similar to high-Ti basalts in the intermediate and outer zones (Xiao et al. 2004). For instance, they show considerable LREE and LILEs enrichment (Fig. 3a, b). However, the high-Ti basalts in the inner zone (Binchuan and Longzhoushan) show some variably geochemical features. The Longzhoushan basalts have compositions closer to the primitive magma

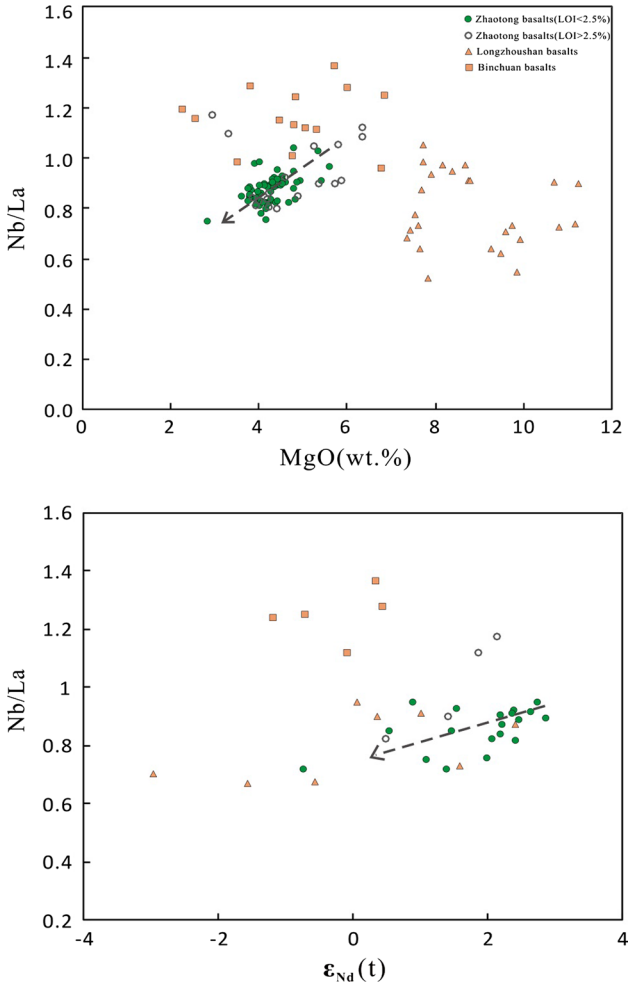

Fig. 7 Plots of Nb/La versus MgO and Nb/La versus ε_{Nd} (*t*) for the Zhaotong basalts, Binchuan basalts and Longzhoushan basalts. Data of the Binchuan samples are from Xiao et al. (2004). The Longzhoushan samples are from Qi et al. (2008)

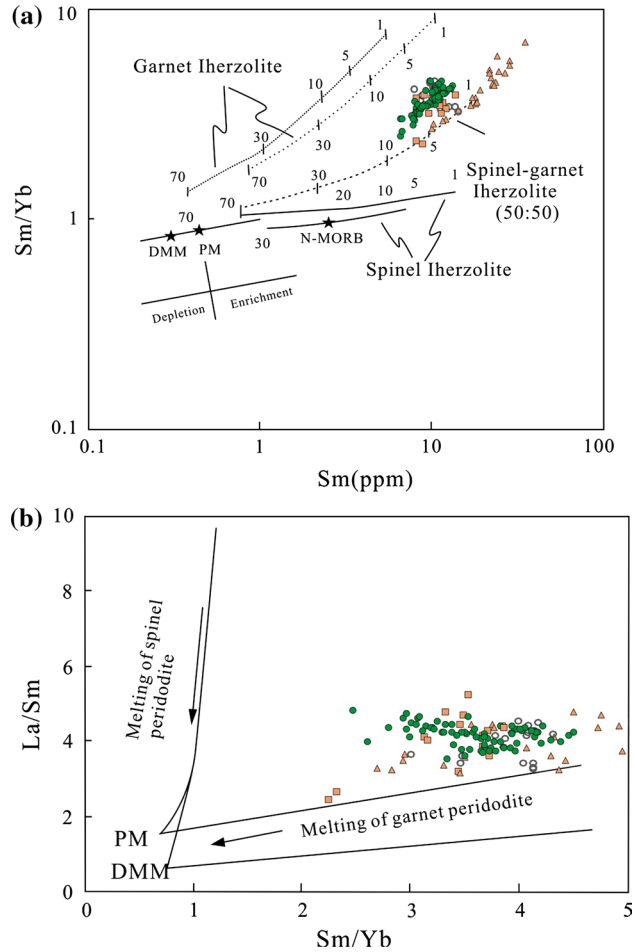

Fig. 8 **a** Plots of Sm/Yb versus Sm for the Zhaotong basalts, Longzhoushan basalts and Binchuan basalts. **b** Plots of La/Sm versus Sm/Yb for the basalts mentioned above. The referred melt curves are after Aldanmaz et al. (2000) and references therein. Primitive mantle (PM) and N-MORB compositions are from Sun and McDonough (1989). Data of the Binchuan samples are from Xiao et al. (2004). The Longzhoushan samples are from Qi et al. (2008). The symbols are the same as those in Fig. 7

according to their relatively higher values of MgO (7.4–11.3 %) and $Mg^{\#}$ (66–53) as well as other compatible elements (Zhong et al. 2006; Qi et al. 2008). By contrast, the Binchuan basalts (HT1) with lower values of MgO (2.26–6.88 %) and $Mg^{\#}$ (31–53) suggest a higher evolution state of the high-Ti magma. The Longzhoushan basalts have lower Nb/La ratios (0.52–1.05) than those (0.96–1.36) of the Binchuan high-Ti basalts and show obvious Nb–Ta negative anomalies and larger range of $\varepsilon_{Nd}(t)$ (−3.0 to +2.4), suggesting involvement of more crustal/SCLM materials. For the Longzhoushan basalts (Fig. 4), the positive corrections between TiO_2, Ni, Cr and MgO, and negative correlation between Al_2O_3 and MgO, indicating that the Longzhoushan basalts may be controlled by fractionation of olivine + clinopyroxene + Ti–Fe oxide. For the Binchuan basalts, TiO_2 and Al_2O_3 show positive relationship with MgO, while there is no clear relationship between Cr, Ni and MgO, suggesting that the Binchuan basalts mainly underwent plagioclase + Ti–Fe oxide fractionation. Besides, the main phenocrysts in the Longzhoushan high-Ti basalts are clinopyroxene, while plagioclase phenocrysts dominate in the Binchuan high-Ti basalts (Xiao et al. 2004; Qi et al. 2008).

Origin of the high-Ti basalts in the ELIP

The origin and mantle source of continental flood basalts are not well constrained and remain the subject of intense debate (He et al. 2010). Numerous models have been proposed to explain the origin of the typical continental flood basalts. For example, there are many authors who have

argued that LIPs are direct results of mantle plume head melting (White and McKenzie 1989; Campbell and Griffiths 1990; Hill 1991), while others have proposed that they result from melting of SCLM which can be caused by heating from a plume (Hawkesworth et al. 1984; Gibson et al. 1995).

The high-Ti basalts in the ELIP have been convinced to form by a mantle plume head. Considerable discussion about these basalts surrounds the extent of contribution of the SCLM and continental crust or recycled crustal materials (Song et al. 2001, 2008; Xiao et al. 2004; Xu et al. 2007; Zhang et al. 2008). Xu et al. (2007) studied Os, Pb and Nd isotope geochemistry in five different areas and proposed that the high-Ti basaltic magmas with low $\gamma_{Os}(t)$ from −0.8 to −1.4 were most likely derived from a SCLM reservoir or were contaminated by a significant amount of lithospheric mantle material during plume-related magma ascent through the SCLM. Further, Lai et al. (2012) suggested the Guangxi basalts represent partial melting of the subcontinental lithospheric mantle and experienced minor crustal contamination during their ascent. However, other workers (e.g., Song et al. 2001, 2008; Xu et al. 2001, 2004; Wang et al. 2007) argued that the high-Ti basalts were generated by low degrees (<8 %) partial melting of the Emeishan mantle plume in the garnet stability field without assimilating subcontinental lithosphere mantle (SCLM) materials.

Our geochemical data are compatible with the idea that the Emeishan high-Ti basalts have a mantle plume origin. However, different geochemical characteristics (as mentioned above) between the high-Ti basalts in the intermediate/outer zones of the ELIP (e.g., Zhaotong, Guizhou, Guangxi and Dashibao) and those in the inner zone (e.g., Binchuan and Longzhoushan) suggest different magmatic processes or mantle sources.

The intermediate and outer zones of the ELIP represent the waning stage of volcanism with a lower mantle temperature and thicker lithosphere, far from the axis of mantle plume, corresponding to their small degrees of partial melting (Xu et al. 2001). Thus, there was not enough heat added to the SCLM to induce SCLM melting and may produce uniform high-Ti basalts with little SCLM contamination (He et al. 2010). All these high-Ti basalts having OIB-like isotopic characteristics and high concentrations of the LREE and LILEs, weak Nb–Ta depletions and invariable $\varepsilon_{Nd}(t)$ among the different areas suggest that the intermediate and outer high-Ti basalts from a homogeneous mantle plume head at garnet-stable depths. There are only minor crustal compositions involved in the magma during their ascent and eruption. Besides, these high-Ti lavas may have experienced extensive plagioclase fractionation in a crustal magma chamber or en route to the surface. This also precludes the possibility of lamproitic melts derived from enriched SCLM as a contaminant of the high-Ti basalts lava in the intermediate and outer zones of the ELIP (Ellam and Cox 1991; Xu et al. 2001).

The high-Ti basalts in the inner zone have more complex geochemical features than those in the intermediate and outer zones of the ELIP. For example, the Binchuan and Longzhoushan basalts are near the center of the ELIP, and they both share OIB-like features (e.g., enrichment of LREE and LILEs), suggesting a deep mantle plume origin. However, they show some distinct geochemical features of major, trace elements and Sr–Nd isotopes as mentioned above. Some Longzhoushan high-Ti basalts show obvious depletions in Nb (Nb/La: 0.52–1.05) while the Binchuan basalts show no negative Nb anomalies (Nb/La: 0.96–1.36), which could be attributed to difference in their mantle source regions or crustal contamination. Both Nb/La versus MgO and Nb/La versus $\varepsilon_{Nd}(t)$ diagrams of the Longzhoushan basalts show no correlations (Fig. 7), indicating a rather heterogeneous mantle source incorporated by crustal/SCLM components rather than crustal contamination during magma ascent. Moreover, the Longzhoushan basalts belong to the HT3 type that show different compositional variations and have been suggested a different mantle source involving crustal/SCLM materials (Xu et al. 2001). Thus, whether the SCLM or crustal materials were involved in the mantle source is important to understand the genesis of the high-Ti basalts in the inner zone (Fig. 8).

Some workers interpret the Emeishan basalts as the products of a Middle/Late Permian mantle plume contaminated by the SCLM beneath the Emeishan large igneous province (ELIP) (Song et al. 2001; Xiao et al. 2003) or mixed with lamproitic magmas from the SCLM (Chung and Jahn 1995). The Re–Os isotopic system is a potentially powerful tool for tracing the origin of magmas in continental settings, because the SCLM typically has lower Os isotopic compositions than the hypothetical primitive upper mantle (Meisel et al. 2001). Besides, both ancient upper and lower crust can be significantly enriched in radiogenic Os. Compared with mantle-derived magmas, γ_{Os} values of the Earth's crust have much higher positive values. Hence, the addition of minor crustal materials would therefore be expected to impart positive γ_{Os} values to the magmas (Zhang 2009). Based on Re–Os isotopic compositions, Xu et al. (2007) proposed that subcontinental lithospheric mantle (SCLM) source was involved in the formation of the Longzhoushan high-Ti basalts according to their low $\gamma_{Os}(t)$ from −0.8 to −1.4. Consequently, the high-Ti basaltic magma was either derived from partial melting of SCLM or contaminated by a significant amount of lithospheric mantle material during plume-related magma ascent through the SCLM. Although we have no information about the exact composition of the SCLM in the inner ELIP, Os isotopic data for harzburgitic mantle from Nushan (Anhui

Province) and Panshishan (Jiangsu Province) in the Yangtze craton suggest the SCLM underlying the ELIP might have strongly negative γ_{Os} (t = 259 Ma) values as low as −10 (Zhi and Qin 2004). Zhang et al. (2008) implied the Lijiang high-Ti/Y picrites (γ_{Os} (t): −0.4 to −2.4) involved minimal amounts of SCLM contamination. They assumed an Emeishan SCLM with 3.4 ppb Os and a γ_{Os} of −10, and picritic melt composition with 2.1 ppb Os and a γ_{Os} of −0.4. The mixing calculations suggest that ~14 % SCLM contamination can account for the entire range in Os isotopic composition of their high-Ti/Y picrites (Zhang et al. 2008). Depleted Os isotope signatures have also been used in other ocean island provinces to indicate involvement of the SCLM. For example, Debaille et al. (2009) measured Os isotopes in lavas from Iceland and Jan Mayen, and found γ_{Os} values similar to those found in the ELIP (as low as −2.1), and they attributed to the presence of the North Atlantic SCLM in the melting zone. Therefore, we believe that SCLM melting remains the most likely way to contribute depleted Os isotope signatures in the ELIP. Moreover, lithospheric signatures for the Longzhoushan high-Ti basalts (γ_{Os}: −0.8 to −1.4) could be more likely involving small amounts of SCLM materials in their mantle source rather than directly melting of the SCLM.

Other workers (Kieffer et al. 2004; Wang et al. 2007) questioned melting of the SCLM. They argued that the lithospheric mantle was not considered to give rise to magmas with diverse chemical characteristics because it is the coldest part of the mantle. Besides, the nature of the SCLM beneath the ELIP is not well constrained, and the degree of melting of the SCLM is not clear. However, recently, Song et al. (2008) studied the Dongchuan area that is closed to the inner zone of the ELIP and suggested that the tephrites in Dongchuan provide first unambiguous evidence for melting of the SCLM in the EILP. They proposed that the tephrites were derived from magmas formed when the base of the previously metasomatized, volatile-mineral-bearing subcontinental lithospheric mantle was heated by the upwelling mantle plume of initial stage. Therefore, the melting of SCLM in the ELIP did occur, and the melting of SCLM should satisfy the following geological conditions: (1) extension and thinning of lithosphere to cause decompression melting; (2) extremely high geotherm; (3) the presence of volatile that can lower the solidus (Kieffer et al. 2004; Xiao et al. 2004).

Shellnutt and Jahn (2011) studied the Emeishan basalts and a mafic dyke in Panzhihua, and they suggested that the high-Ti basalts were intruded by the ~260 Ma Panzhihua gabbroic complex. Thus, these high-Ti basalts may erupt slightly earlier than the mafic intrusion. In the Longhzoushan area, the high-Ti basalts were underlain by low-Ti basalts (Xu et al. 2007; Qi and Zhou 2008), indicating the high-Ti basalts might erupt earlier than the low-Ti basalts. The high-Ti basalts are considered to be the parental magmas of the Fe–Ti oxide bearing gabbros, while the low-Ti basalts are thought to be the parental magmas of Ni–Cu sulfide deposits (Wang et al. 2007; Zhou et al. 2008). Besides, the ELIP Fe–Ti oxide deposits are merely concentrated within the inner zone, while the Ni–Cu sulfide deposits are located within the whole ELIP. Shellnutt and Jahn (2010) have successfully modeled the genesis of two Fe–Ti oxide deposits using high-Ti basalts. Therefore, high-Ti basalts in the inner zone may have erupted during the early stages of the ELIP volcanism rather than the waning stages (Shellnutt and Jahn 2011). Thus, the high-Ti magma in the inner zone may have much higher geotherm than that in the intermediate and outer zones. Moreover, Xu et al. (2001) suggested the high-Ti magmas were probably volatile-rich, as evidenced by the presence of primary biotite in these rocks. The rising mantle plume head could also cause extension and thinning of lithosphere, and further decompression melting of the SCLM. Therefore, these features fulfilled the conditions required for melting of small quantities of SCLM in the inner zone of the ELIP, and the different geochemical characteristics of these high-Ti basalts might be due to the heterogeneous mantle source that entrapped some melting SCLM materials.

Overall, the high-Ti basalts in the ELIP originated from the mantle plume head. At the periphery of the Emeishan plume head, where the mantle source is rather homogenous, the lithospheric lid was thicker and the temperature was lower, low degrees of melting in the garnet stability field formed the uniform Emeishan high-Ti basalts in the intermediate and outer zones of the ELIP. By contrast, the high-Ti basalts in the inner zone are near the center of the ELIP, where the lithospheric lid was thinner and geotherm was higher, thus the heterogeneous mantle source that involved some SCLM materials contributed to variably geochemical characteristics of the basalts. However, we cannot entirely rule out the involvement of the crustal materials in the formation of the inner high-Ti basalts, because only limited Os data have been obtained in the ELIP, and interaction processes between the Emeishan mantle plume and lithosphere are more complex than we thought. Thus, further more studies (e.g., Re–Os isotopes) in the ELIP are required to better understand whether the geochemical differences of these basalts are controlled by these dependent or independent processes that took place in different parts of the plume and SCLM.

Conclusions

All samples collected from Zhaotong belong to the high-Ti group basalts. Petrological and geochemical characteristics of the Zhaotong basalts indicate that they originated

from less than 8 % partial melting of a garnet-dominated peridotite, OIB-like mantle source and experienced limited crustal contamination. The high-Ti basalts in the intermediate and outer zones of the ELIP share many similarities in elemental and Sr–Nd isotopic geochemistry, indicating that they originated directly from the Emeishan mantle plume and formed by large scale and low degrees of partial melting. In contrast, the basalts in the inner zone of the ELIP exhibit different characteristics and suggest that these high-Ti basalts represent partial melting of a mantle plume head that entrapped some SCLM materials when the upwelling of plume triggered partial melting of the SCLM.

Acknowledgments The authors appreciate the assistance of Jing Hu, Jing Wang and Fang Xiao with elements and Sr–Nd isotope measurement at Institute of Geochemistry, Chinese Academy of Science. Gaoliang Li is thanked for the help in field work. This study is jointly supported by the National Basic Research Program of China (2014CB440903) and the National Natural Science Foundation of China (41425011).

References

Aldanmaz E, Pearce JA, Thirlwall MF et al (2000) Petrogenetic evolution of late Cenozoic, post-collision volcanism in western Anatolia, Turkey. J Volcanol Geotherm Res 102:67–95

Ali JR, Gary MT, Zhou MF et al (2005) Emeishan large igneous province, SW China. Lithos 79:475–489

Bezard R, Davidson JP, Turner S et al (2014) Assimilation of sediments embedded in the oceanic arc crust: myth or reality? Earth Planet Sci Lett 395:51–60

Campbell IH, Griffiths RW (1990) Implications of the mantle plume structure for the evolution of flood basalts. Earth Planet Sci Lett 99:79–93

Chen JF, Jahn BM (1998) Crustal evolution of southeastern China: Nd and Sr isotopic evidence. Tectonophysics 284:101–133

Chen Y, Xu YG, Xu T et al (2015) Magmatic underplating and crustal growth in the Emeishan Large Igneous Province, SW China, revealed by a passive seismic experiment. Earth Planet Sci Lett 432:103–114

Chung SL, Jahn BM (1995) Plume-lithosphere interaction in generation of the Emeishan flood basalts at the Permian-Triassic boundary. Geology 23:889–892

Chung SL, Jahn BM, Wu GY et al (1998) The Emeishan flood basalt in SW China: a mantle plume initiation model and its connection with continental break-up and mass extinction at the Permian–Triassic boundary. In: Flower MFJ, Chung S-L, Lo C-H, Lee T-Y (eds) Mantle dynamics and plate interaction in East Asia. Geodynamics series, vol 27. American Geophysical Union, Washington, DC, pp 47–58

Debaille V, Trønnes RG, Brandon AD et al (2009) Primitive off-rift basalts from Iceland and Jan Mayen: Os-isotopic evidence for a mantle source containing enriched subcontinental lithosphere. Geochim Cosmochim Acta 73:3423–3449

Ellam RM, Cox K (1991) An interpretation of Karoo picrite basalts in terms of interaction between asthenospheric magmas and the mantle lithosphere. Earth Planet Sci Lett 105:330–342

Fan WM, Zhang CH, Wang YJ et al (2008) Geochronology and geochemistry of Permian basalts in western Guangxi Province, Southwest China: evidence for plume-lithosphere interaction. Lithos 102:218–236

Frey FA, Garcia MO, Wise WS et al (1993) The evolution of Mauna Kea volcano, Hawaii: petrogenesis of tholeiitic and alkali basalts. J Geophys Res 96:14347–14375

Gao S, Lin WL, Qiu YM et al (1999) Contrasting geochemical and Sm–Nd isotopic compositions of Archaean metasediments from the Kongling high-grade terrain of the Yangtze craton: evidence for cratonic evolution and redistribution of REE during crustal anatexis. Geochim Cosmochim Acta 63:2071–2088

Gibson SA, Thompson RN, Dickin AP et al (1995) High-Ti and low-Ti mafic potassic magmas: key to plume-lithosphere interactions and continental flood-basalt genesis. Earth Planet Sci Lett 136:149–165

Hao YL, Zhang ZC, Wang FS et al (2004) Petrogenesis of high-Ti and low-Ti basalts from the Emeishan large province. Geol Rev 50(6):587–592 **(in Chinese with English abstract)**

Hawkesworth CJ, Rogers NW, Van Calsteren PWC, Menzies MA (1984) Mantle enrichment processes. Nature 311:331–335

He B, Xu YG, Xiao L et al (2003) Sedimentary evidence for a rapid, kilometer-scale crustal doming prior to the eruption of the Emeishan flood basalts. Earth Planet Sci Lett 213:391–405

He Q, Xiao L, Brian B et al (2010) Variety and complexity of the Late-Permian Emeishan basalts: reappraisal of plume–lithosphere interaction processes. Lithos 199:91–107

Hellebrand E, Snow JE, Hoppe P, Hofmann AW (2002) Garnet-field melting and late stage fertilization in "Residual" abyssal peridotites from the central indian ridge. J Petrol 43:2305–2338

Hill RI (1991) Starting plumes and continental break-up. Earth Planet Sci Lett 104:398–416

Jahn BM, Wu FY, Lo CH et al (1999) Crust-mantle interaction induced by deep subduction of the continental crust: geochemical and Sr-Nd isotopic evidence from post-collisional mafic-ultramafic intrusions of the northern Dabie complex, central China. Chem Geol 157:119–146

Kieffer B, Arndt NT, Lapierre H et al (2004) Flood and shield basalts from Ethiopia: magmas from the African superswell. J Petrol 45:793–834

Lai SC, Qin JF, Li YF et al (2012) Permian high Ti/Y basalts from the eastern part of the Emeishan Large Igneous Province, southwestern China: petrogenesis and tectonic implications. J Asian Earth Sci 47:216–230

Ma CQ, Ehlers C, Xu CH et al (2000) The roots of the Dabieshan ultrahigh-pressure metamorphic terrain: constraints from geochemistry and Nd–Sr isotope systematics. Precambrian Res 102:279–301

MacDonald GA, Katsura T (1964) Chemical composition of Hawaiian lavas. J Petrol 5:82–133

McKenzie D, O'Nions RK (1991) Partial melt distributions from inversion of rare Earth element concentrations. J Petrol 32:1021–1091

Meisel T, Walker RJ, Irving AJ et al (2001) Osmium isotopic compositions of mantle xenoliths: a global perspective. Geochim Cosmochim Acta 65:1311–1323

Qi L, Zhou MF (2008) Platinum-group elemental and Sr-Nd-Os isotopic geochemistry of Permian Emeishan flood basalts in Guizhou Province, SW China. Chem Geol 248:83–103

Qi L, Hu J, Gregoire DC (2000) Determination of trace elements in granites by inductively coupled plasma mass spectrometry. Talanta 51:507–513

Qi L, Wang CY, Zhou MF (2008) Controls on the PGE distribution of Permian Emeishan alkaline and peralkaline volcanic rocks in Longzhoushan, Sichuan Province, SW China. Lithos 106(3–4):222–236

Shellnutt JG, Jahn BM (2010) Formation of the Late Permian Panzhihua plutonic-hypabyssal-volcanic igneous complex: implications for the genesis of Fe–Ti oxide deposits and A-type granites of SW China. Earth Planet Sci Lett 289:509–519

Shellnutt JG, Jahn BM (2011) Origin of Late Permian Emeishan basaltic rocks from the Panxi region (SW China): implications for the Ti-classification and spatial-compositional distribution of the Emeishan flood basalts. J Volcanol Geotherm Res 199:85–95

Song XY, Zhou MF, Hou ZQ et al (2001) Geochemical constraints on the mantle source of the upper Permian Emeishan continental flood basalts, southern China. Int Geol Rev 43:213–225

Song XY, Zhou MF, Cao ZM et al (2004) Late Permian rifting of the South China Craton caused by the Emeishan mantle plume. J Geol Soc Lond 161:773–781

Song XY, Zhou MF, Keays RR et al (2006) Geochemistry of the Emeishan flood basalts at Yangliuping, Sichuan, SW China: implication for sulfide segregation. Contrib Miner Petrol 152:53–74

Song XY, Qi HW, Robinson PT et al (2008) Melting of the subcontinental lithospheric mantle by the Emeishan mantle plume: evidence from the basal alkaline basalts in Dongchuan, Yunnan, Southwestern China. Lithos 100:93–111

Song XY, Keays RR, Xiao L et al (2009) Platinum-group element geochemistry of the continental flood basalts in the central Emeisihan Large Igneous Province, SW China. Chem Geol 15656:1–16

Sun SS, McDonough WF (1989) Chemical and isotopic systematics of oceanic basalts: implications for mantle composition and processes. In: Saunders AD, Norry MJ (eds) Magmatism in the Ocean Basins: Geological Society, vol 42. Special Publications, London, pp 313–345

Wang CY, Zhou MF, Qi L (2007) Permian flood basalts and mafic intrusions in the Jinping (SW China)–Song Da (northern Vietnam) district: mantle sources, crustal contamination and sulfide segregation. Chem Geol 243:317–343

White R, McKenzie D (1989) Magmatism at rift zones: the generation of volcanic continental margins and flood basalts. J Geophys Res 94:7685–7729

Wilson M (1989) Igneous petrogenesis. Unwin Hyman, London, pp 245–285

Xiao L, Xu YG, Chung SL et al (2003) Chemostratigraphic correlation of Upper Permian lava succession from Yunnan Province, China: extent of the Emeishan igneous province. Int Geol Rev 45:753–766

Xiao L, Xu YG, Mei HJ et al (2004) Distinct mantle sources of low-Ti and high-Ti basalts from the western Emeishan large igneous province, SW China: implications for plume-lithosphere interaction. Earth Planet Sci Lett 228:525–546

Xu YG, He B (2007) Thick and high velocity crust in Emeishan large igneous province, SW China: evidence for crustal growth by magmatic underplating/intraplating. The Origins of Melting Anomalies: Plates, Plumes, and Planetary Processes, edited by G Foulger and D Jurdy. Geol Soc Am Spec Pub 430:841–858

Xu YG, Chung SL, Jahn BM et al (2001) Petrologic and geochemical constraints on the petrogenesis of Permian-Triassic Emeishan flood basalts in southwestern China. Lithos 58:145–168

Xu YG, He B, Chung SL et al (2004) The geologic, geochemical and geophysical consequences of plume involvement in the Emeishan flood basalt province. Geology 30:917–920

Xu JF, Suzuki K, Xu YG et al (2007) Os, Pb, and Nd isotope geochemistry of the Permian Emeishan continental flood basalts: insights into the source of a large igneous province. Geochim Cosmochim Acta 71:2104–2119

Xu T, Zhang ZJ, Liu BF et al (2015) Crustal velocity structure in the Emeishan Large Igneous Province and evidence of the Permian mantle plume activity. Sci China 58:1133–1147

Yan DP, Zhou MF, Song HL et al (2003) Origin and tectonic significance of a Mesozoic multi-layer over-thrust system within the Yangtze Block (South China). Tectonophysics 361:239–254

Zhang ZC (2009) A discussion on some important problems concerning the Emeishan large province. Geol China 36(3):634–646 **(in Chinese with English abstract)**

Zhang ZC, Mahoney JJ, Mao JW et al (2006) Geochemistry of picritic and associated basalt flows of the western Emeishan flood basalt province, China. J Petrol 47:1997–2019

Zhang ZC, Zhi XC, Chen L et al (2008) Re–Os isotopic compositions of picrites from the Emeishan flood basalt province, China. Earth Planet Sci Lett 276:30–39

Zhi XC, Qin X (2004) Re-Os isotope geochemistry of mantle-derived peridotite xenoliths from eastern China: constraints on the age and thinning of the lithosphere mantle. Acta Petrol Sin 20:989–998

Zhong H, Zhou XH, Zhou MF et al (2002) Platinum-group element geochemistry of the Hongge layered Intrusion in the Pan-Xi area, south western China. Miner Depos 37:226–239

Zhong H, Zhu WG, Qi L et al (2006) Platinum-group element (PGE) geochemistry of the Emeishan basalts in the Pan-Xi area, SW China. Chin Sci Bull 51:845–854

Zhong H, Qi L, Hu RZ et al (2011) Rhenium–osmium isotope and platinum-group elements in the Xinjie layered intrusion, SW China: implications for source mantle composition, mantle evolution, PGE fractionation and mineralization. Geochim Cosmochim Acta 75:1621–1641

Zhong YT, He B, Mundil R et al (2014) CA-TIMS zircon U-Pb dating of felsic ignimbrite from the Binchuan section: implications for the termination age of Emeishan large igneous province. Lithos 204:14–19

Zhou MF, Malpas J, Song XY et al (2002) A temporal link between the Emeishan large igneous province (SW China) and the end-Guadalupian mass extinction. Earth Planet Sci Lett 196:113–122

Zhou MF, Robinson PT, Lesher CM et al (2005) Geochemistry, petrogenesis and metallogenesis of the Panzhihua gabbroic layered intrusion and associated Fe-Ti-V oxide deposits, Sichuan province, SW China. J Petrol 46:2253–2280

Zhou MF, Arndt NT, Malpas J et al (2008) Two magma series and associated ore deposit types in the Permian Emeishan large igneous province, SW China. Lithos 103:352–368

Zi JW, Fan WM, Wang JY et al (2010) U-Pb geochronology and geochemistry of the Dashibao basalts in the Songpan-Ganzi terrane, SW China, with implications for the age of Emeishan volcanism. Am J Sci 210:1054–1080

Zindler A, Hart SR (1986) Chemical geodynamics. Ann Rev Earth Planet Sci Lett 14:493–571